

# MSMD-Net: Deep Stereo Matching with Multi-scale and Multi-dimension Cost Volume

Zhelun Shen<sup>1,2</sup>, Yuchao Dai<sup>1\*</sup>, Zhibo Rao<sup>1</sup>

<sup>1</sup> Northwestern Polytechnical University

<sup>2</sup> Peking University

shenzhelun@pku.edu.cn, daiyuchao@nwpu.edu.cn, raoxi36@foxmail.com

## Abstract

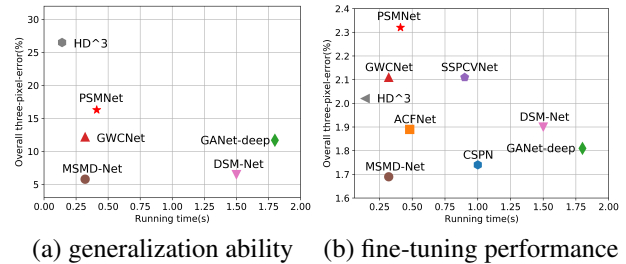
Deep end-to-end learning based stereo matching methods have achieved great success as witnessed by the leaderboards across different benchmarking datasets (KITTI, Middlebury, ETH3D, etc). However, real scenarios not only require approaches to have state-of-the-art performance but also real-time speed and domain-across generalization, which cannot be satisfied by existing methods. In this paper, we propose MSMD-Net (Multi-Scale and Multi-Dimension) to construct *multi-scale* and *multi-dimension* cost volume. At the multi-scale level, we generate four 4D combination volumes at different scales and integrate them with an encoder-decoder process to predict an initial disparity estimation. At the multi-dimension level, we additionally construct a 3D warped correlation volume and use it to refine the initial disparity map with residual learning. These two dimensional cost volumes are complementary to each other and can boost the performance of disparity estimation. Additionally, we propose a switch training strategy to alleviate the overfitting issue appeared in the pre-training process and further improve the generalization ability and accuracy of final disparity estimation. Our proposed method was evaluated on several benchmark datasets and ranked first on KITTI 2012 leaderboard and second on KITTI 2015 leaderboard as of September 9. In addition, our method shows strong domain-across generalization and outperforms best prior work by a noteworthy margin with three or even five times faster speed. The code of MSMD-Net is available at <https://github.com/gallenszl/MSMD-Net>.

## Introduction

Stereo matching aims at estimating the disparity map between a rectified image pair, which is of great importance to various applications such as autonomous driving (Chen et al. 2015) and robotics navigation (Biswas and Veloso 2011). Recently, the unprecedented advancement of deep learning in high level vision tasks has been extended to geometric problems such as stereo matching. Currently, deep end-to-end learning-based approaches have achieved state-of-the-art performance on most of the standard stereo matching benchmarks, i.e., KITTI, Middlebury and ETH3D.

Copyright © 2021, Association for the Advancement of Artificial Intelligence (www.aaai.org). All rights reserved.

\* Corresponding Author



(a) generalization ability (b) fine-tuning performance

Figure 1: Plots comparing generalization ability and fine-tuning performance vs inference time on KITTI 2015. Left: generalization ability vs inference time on KITTI2015 training sets without fine-tuning. Right: fine-tuning performance vs inference time on KITTI2015 test sets..

However, real scenarios not only require approaches to have state-of-the-art performance but also real-time speed and domain-across generalization. Existing state-of-the-art methods (Cheng, Wang, and Yang 2019; Zhang et al. 2020) cannot meet this demand, which only focus on one or two aspects and cannot make a good trade-off between all these requirements. Thus, a key challenge for further research is designing an architecture that perform better, run faster and generalize well to novel scenes jointly.

To tackle above problems, we introduce MSMD-Net to construct multi-scale and multi-dimension cost volume. MSMD-Net enjoys the following strengths:

- *State-of-the-art accuracy with high efficiency:* On KITTI2015, MSMD-Net achieves 1.69% 3-pixel error rate, a 2.87% error reduction from best published method with 3 times faster speed (Comparing with 3.87% error reduction from former best published method). On KITTI2012, MSMD-Net achieves 1.37% overall three-pixel-error rate, an 11.04% error reduction from best published method with similar speed (Comparing with 3.75% error reduction from former best published method).
- *Strong generalization:* When only trained on same synthetic dataset (Scene Flow), MSMD-Net get an 5.6% three-pixel-error rate on KITTI 2015, a 13.85% error reduction from best prior network. On KITTI2012, MSMD-Net achieves 4.2% three-pixel-error rate, a 32.26% error reduction from best prior network. On ETH3D, MSMD-

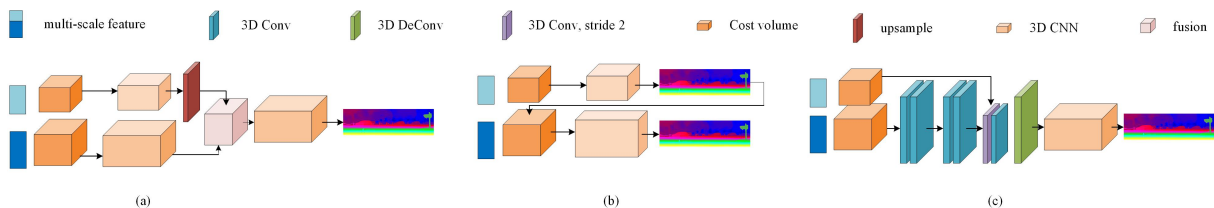


Figure 2: Comparison between different methods of employing multi-scale cost volume. (a) SSPCV (Wu et al. 2019), (b) cascade volume (Cheng et al. 2019; Gu et al. 2020; Yang et al. 2020) and (c) our proposed cost volume integration module. Note that, to simplify the illustration, we assume that all methods only use two different scale cost volumes. Extension the number of cost volume is straightforward. We also omit the skip connection for better visual contrast.

Net achieves 5.2% one-pixel-error rate, a 16.13% error reduction from best prior network.

MSMD-Net consists of three parts: a feature extraction that extracts multi-scale features for subsequent cost volume construction, a cost volume integration that fuses 4D multi-scale cost volume to generate the initial disparity, a geometry guidance disparity refinement that constructs 3D warped cost volume to refine the initial disparity by employing geometry of stereo vision. These two dimensional cost volumes are complementary to each other and can boost the performance and generalization of disparity estimation.

The design of MSMD-Net draws inspiration from many existing works but is substantially novel. First, MSMD-Net constructs multi-scale cost volumes respectively. In contrast, existing methods only build a single cost volume at a fixed resolution. By employing multi-scale cost volumes, our method can better exploit global context information and enlarge the receptive fields to capture more robust structural cues and reduce the dependence on domain-sensitive local cues, which also facilitates the estimation of ill-posed regions such as repeated patterns. While it is noteworthy that the insight of employing multi-scale cost volume has also been investigated in (Gu et al. 2020; Yang et al. 2020; Wu et al. 2019), our work differs from theirs in the following two main aspects: 1) We build multi-scale cost volume explicitly with both feature concatenation and group-wise correlation, which is more discriminative than single feature concatenation; 2) (Gu et al. 2020; Yang et al. 2020) propose cascade volume to respectively use multi-scale cost volume and iteratively narrow the disparity range and refine depth maps in a coarse-to-fine manner. SSPCV (Wu et al. 2019) integrates the multi-scale cost volume by gradually upsampling the lowest scale to the highest. However, these two methods both have several drawbacks. The cascade volume loses much information during the process of narrowing down the disparity searching range and SSPCV needs a long inference time to constantly employ 3D hourglass modules to regularize the upsampled cost volume. Instead, we design a cost volume integration module to fuse multi-scale cost volume in an encoder-decoder process, which preserves the whole disparity range and decreases the number of 3D hourglass modules at the same time. The visual comparison can be seen in Figure 2.

Second, the disparity refinement module of MSMD-Net owns geometry guidance. The insight of disparity refine-

ment has been investigated in many deep stereo matching methods. For these previous work, they mainly depend on the network to automatically learn a map between input information and residue without employing the geometry of stereo vision. In contrast, we propose a warped correlation volume to define a fine-grained disparity searching range between initial disparity map and ground-truth, which makes network can easier to find the corresponding pixel-level residue.

Third, we introduce a novel switch training strategy to alleviate the overfitting issues appeared when extending the pre-training process on the Scene Flow datasets. Experiments have shown the effectiveness of our switching training strategy compared with using a single activation function.

We conduct experiments on several benchmark datasets and ranked first on KITTI 2012 leaderboard and second on KITTI 2015 leaderboard as of September 9. In addition, figure 1 further demonstrates our method make a good trade-off between performance, speed and generalization.

## Related Work

### End-to-end deep stereo matching without refinement:

Estimating depth from a rectified image pair is a classical problem which has been studied for decades. DispNet (Mayer et al. 2016) is a real breakthrough which first proposes to construct a correlation cost volume and directly progresses the disparity map in an end-to-end way. Other than DispNet, GCNet (Kendall et al. 2017) proposes to construct concatenation volume and regularize it with 3D convolution layers. GWCNet (Guo et al. 2019) introduces group-wise correlation to provide better similarity measures than previous work and it can cooperate with the concatenation volume to further improve the performance. Following these work, (Liang et al. 2019a; Aleotti et al. 2020) propose to push unsupervised stereo matching and ACFNet (Zhang et al. 2019b) solves the uncertain distribution of cost volume by directly using unimodal ground truth distributions to supervise cost volume. For all these prior work, cost volume construction has been placed in an extremely important position and deserves further exploration

**End-to-end deep stereo matching with refinement:** Recently, many researchers Pang et al.; Tonioni et al.; Sun et al.; Liang et al.; Duggal et al. attempt to integrate the disparity refinement step into an end-to-end learning model. (Pang et al. 2017) introduce a two-stage network called CRL

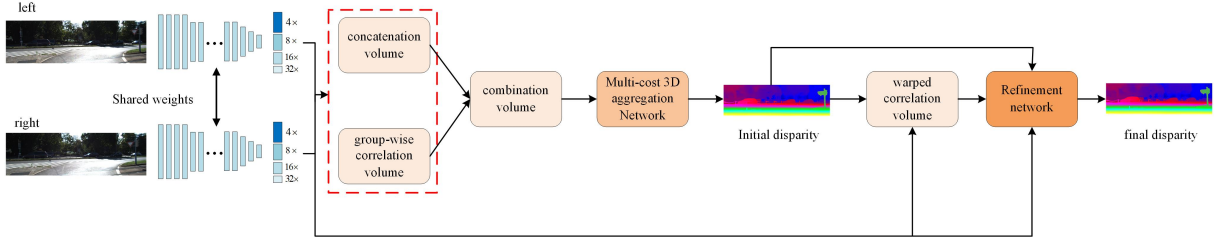


Figure 3: Network architecture of our proposed framework, which consists of 3 consecutive modules: feature extraction, 4D multi-scale combination volume for cost aggregation and 3D warped correlation volume for disparity refinement.

in which the first stage extends DispNet (Mayer et al. 2016) to get an initial disparity map with more details and the second stage refines the initial disparity map in a residual manner. Different from CRL, (Liang et al. 2019b) propose to calculate reconstruction error in feature space rather than colour space and share features between disparity estimation network and refinement network. (Sun et al. 2018) propose a context network, which is based on dilated convolutions to refine flow. Different from these work, here we introduce the warped correlation cost volume to guide the disparity refinement. Specifically, the warped correlation cost volume defines a fine-grained disparity searching range by warping right image features to left image features according to a pre-defined residue range. Comparing with directly regressing a residue with context information, the warped correlation significantly alleviates the difficulty of network to find the corresponding pixel-level residue.

**End-to-end deep stereo matching using multi-scale information:** Multi-scale information has been widely employed in stereo estimation. PSM-Net (Chang and Chen 2018) introduces SPP module to generate feature maps at different levels. (Liang et al. 2019b) proposes a shallow encoder-decoder architecture to extract multi-scale features of the original picture. However, most existing work only use multi-scale features to construct a single volume at a fixed resolution other than considering them separately. Some work (Yang et al. 2020; Gu et al. 2020; Cheng et al. 2019; Wu et al. 2019) also discover this issue and give some solutions to employ multi-scale cost volume. (Yang et al. 2020; Gu et al. 2020; Cheng et al. 2019) propose to construct cascade multi-scale cost volume and progressively regress a high-quality disparity map from the coarsest cost volume. Comparing with estimating disparity map at each scale respectively, our work introduces an encoder-decoder process to directly integrate different scale cost volumes to capture more robust global feature representation for the regularization of cost volume. Our method also shares similarities with SSPCV (Wu et al. 2019). However, SSPCV just fuses multi-scale cost volumes by constantly employing 3D hourglass modules to regularize the upsampled cost volume, which is time-consuming and GPU memory-unfriendly.

## Our Approach

This section describes the details of our method to construct multi-scale and multi-dimension cost volume. An overview of our approach is illustrated in Figure 3, which consists of

three parts: feature extraction, 4D multi-scale combination volume for cost aggregation, 3D warped correlation volume for disparity refinement. Our feature extraction is a little similar to the Resnet-like network proposed in (Guo et al. 2019) but employing three more residual blocks with stride 2 to get feature maps at different scales (see Supplementary material for more information). And the details of the other two parts will be introduced below.

### 4D Multi-scale Combination Volume for Cost Aggregation

We propose to construct multi-scale combination volumes and integrate them with an encoder-decoder process for initial disparity estimation. Specifically, we employ the extracted multi-scale feature to construct combination volume, which is constituted of concatenation volume and group-wise correlation volume. We denote the extracted multi-scale feature as  $f^i$ , where  $i$  means the  $i^{th}$  scale and  $i = 1$  represents the highest scale (1/4 of the original input image resolution). The concatenation volume is computed as:

$$V_{concat}^i(d, x, y, f) = f_L^i(x, y) \parallel f_R^i(x - d, y), \quad (1)$$

where  $\parallel$  denotes the vector concatenation operation at the feature dimension and group-wise correlation volume is computed as:

$$V_{gwc}^i(d, x, y, g) = \frac{1}{N_c^i/N_g} \langle f_l^{ig}(x, y), f_r^{ig}(x - d, y) \rangle \quad (2)$$

where  $N_c$  represents the channels of the extracted feature.  $N_g$  is the number of group and  $\langle \cdot, \cdot \rangle$  represents the inner product. We use the concatenation operation to get final multi-scale combination volume

$$V_{combine}^i = V_{concat}^i \parallel V_{gwc}^i. \quad (3)$$

Note that when generating group-wise correlation volume, compared with GWCNet, we add one more convolution layer without activation function and batch normalization to make it own the same data distribution with concatenation volume. It optimizes the combination volume and makes it suitable for all datasets so we don't need to use different cost volumes to fit different datasets like GWCNet. Then the multi-scale combination volume will be employed for cost aggregation.

The stacked hourglass architecture (Guo et al. 2019; Zhang et al. 2019b) has shown its efficiency in cost aggregation and we extend the stacked hourglass architecture with

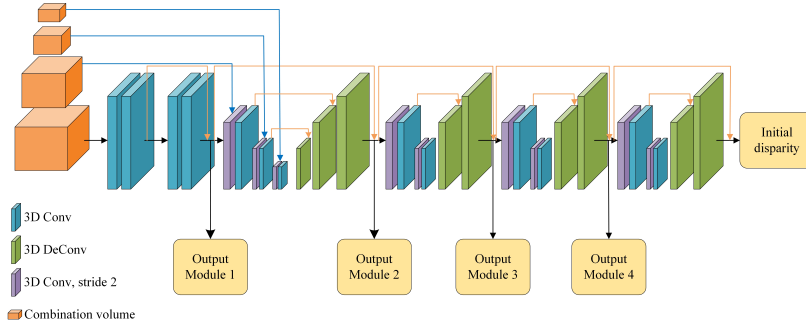


Figure 4: Detailed structure of our multiple cost 3D aggregation network. Compared with GWCNet, it adds an additional cost volume integration module to merge different scale cost volumes. Note that the output module is only be applied during the training process.

a cost volume integration module to employ multi-scale 4D combination volumes. As shown in Figure 4, the architecture of our cost volume integration module is similar to the hourglass network for maintaining a uniform structure. Additionally, we extend the original architecture to  $1/32$  the size of the original image and integrate corresponding scale combination volume into the down-sampled cost volume by concatenation operation at the feature dimension (see blue lines in Figure 4). Specifically, we first employ a 3D convolution layer with stride two to downsample the first scale combination volume ( $1/4$  of the original input image size) to  $1/8$  of the original input image size. Then we concatenate the down-sampled cost volume and the second scale combination volume at the feature dimension and use one additional 3D convolution layer to decrease the feature channel to a fixed size. Similar operation is progressively employed until we downsample the cost volume to  $1/32$  of the original input image size. Finally, 3D transposed convolution is employed to progressively up-sample the volume to  $1/4$  of the original input image size. The feature dimension is set as 32, 64, 128, 128 from the first scale to the last and the  $1 \times 1 \times 1$  3D convolution in the shortcut connection is still preserved to improve the performance (see yellow lines in Figure 4). Then we use three stacked 3D hourglass networks to further regularize and refine the volume. Finally, an output module is employed to predict the disparity. The output module uses two more 3D convolution layers to get a 1-channel 4D volume, then it upsamples the 1-channel 4D volume to the original image resolution ( $H \times W \times D$ ) and applies soft argmin operation (Kendall et al. 2017) to generate initial disparity map.

### 3D Warped Correlation Volume for Disparity Refinement

We construct 3D warped correlation volume to generate a fine-grained disparity searching range for disparity refinement. Specifically, the 3D warped correlation volume is generated by the left feature and warped right feature. The disparity residue between left feature and warped right feature is usually small so we can define a smaller disparity searching range to refine the initial disparity map with fine-grained correspondences. The warping operation is implemented differentially by bilinear sampling (Jaderberg et al.

2015). The 3D warped correlation volume is computed as:

$$V_{warpedcorr}(d, x, y) = \frac{1}{N_c} \langle f_l(x, y), f_{wr}(x - d, y) \rangle \quad (4)$$

where  $f_l$  and  $f_{wr}$  are upsampled from the first scale feature to the original image resolution. Note that the warped correlation volume measures the similarities between left feature and reconstructed left feature (warped right feature) at each disparity level. We hope the network can pick out the most similar disparity level with the help of context information. This approach significantly alleviates the difficulty of network to find the corresponding pixel-level residue comparing with directly regressing the residue by context information without any geometry correspondence. In addition, the warped correlation volume is a 3D cost volume ( $H \times W \times D$ ), compared with 4D combination volume, such design makes it possible to be regularized at the original image resolution with an acceptable run-time and GPU memory.

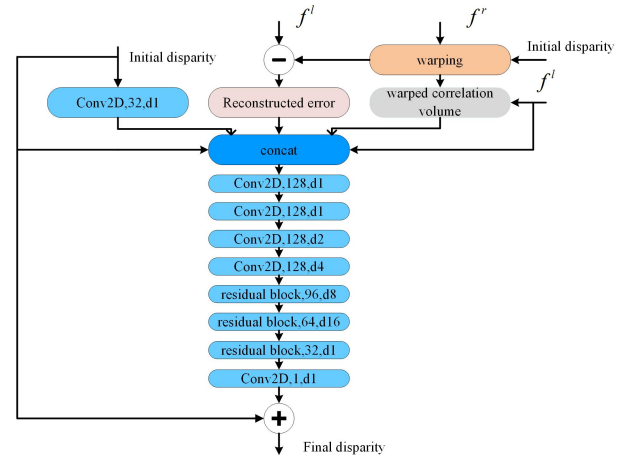


Figure 5: Detailed structure of our refinement network. The network consists of four convolution layers, three basic residual blocks and another one convolution layer (without BN/Relu). Note that the dilation rate is defined as  $d$  followed by the value.

All in all, we use the warped correlation volume, initial disparity map, left feature and reconstructed error as the in-

put of our refinement network. Compared with directly using initial disparity, we use a convolution layer to generate a 32-channel initial disparity feature map to increase the weight of initial disparity map in the input formation. In addition, the reconstructed error is computed by the left feature and the warped right feature as:

$$E_{reconstruct} = f_l(x, y) - f_{wr}(x, y). \quad (5)$$

The architecture of our refinement network is shown in Figure 5. We use a dilated convolution (Yu and Koltun 2015) based network to enlarge the receptive field so that network can be more robust and better refine low-texture ambiguities. Specifically, it is composed of 5 convolution layers and three basic residual blocks with different dilation constants. The dilation constants are 1,1,2,4,8,16,1 and 1 from top to bottom.

Compared with previous work, the input of our network is more interpretable. The warped correlation volume identifies a fine-grained disparity searching range between initial disparity map and ground truth. The reconstructed error shows the incorrect regions which should be improved in the refinement step. The initial disparity map gives a baseline of our disparity estimation and the left feature contains enough context informing for residual learning. Reconstructed error, initial disparity map, and left feature cooperate with each other to support the network to find the most similar disparity level in the warped correlation volume at pixel-wise level.

## Loss Function

We employ smooth  $L_1$  loss function to train our network in an end-to-end way. For each submodule in 3D cost aggregation, same output module and soft argmin operation are used to get intermediate disparity map. In total, we get six disparity maps  $d_0, d_1, d_2, d_3, d_4, d_5, d_6$  and the loss function is described as:

$$L = \sum_{i=0}^{i=5} w_i \cdot Smooth_{L_1}(d_i - \hat{d}) \quad (6)$$

in which

$$Smooth_{L_1}(x) = \begin{cases} 0.5x^2, & \text{if } |x| < 1 \\ |x| - 0.5, & \text{otherwise} \end{cases} \quad (7)$$

where  $\hat{d}$  represents the ground-truth disparity and  $w_i$  is the weight of the  $i^{th}$  estimation of disparity map.

## Experiment

In this section, we evaluate our proposed model on three datasets: Scene Flow (Mayer et al. 2016), ETH3D (Schops et al. 2017) and KITTI datasets (Geiger, Lenz, and Urtasun 2012a,b) and compare it with several state-of-the-art architectures. We also employ ablation studies to evaluate the influence of the proposed cost volume representation. Furthermore, we introduce a novel training strategy with a switch between two different activation functions.

## Dataset

**SceneFlow:** This is a large synthetic dataset with 35,454 training and 4,370 test images of size  $960 \times 540$  for optical flow and stereo matching. It is composed of Flyingthings3D, Driving, and Monkaa with dense and accurate ground-truth for training. We use the Finalpass of the Scene Flow datasets to pre-train our network.

**ETH3D:** ETH3D is a grayscale image dataset with both indoor and outdoor scenes. It contains 27 training and 20 testing image pairs with sparsely labeled ground-truth. We use the 27 training image pairs to evaluate the generalization of our network.

**KITTI 2015 & KITTI 2012:** These two datasets are both real-world dataset collected from a driving car. KITTI 2015 contains 200 training and another 200 testing image pairs while KITTI 2012 provides 194 training and another 195 testing image pairs. Every training image pair is provided a sparse ground-truth disparity collected using LIDAR. For both datasets, we use 180 training image pairs as a training set and the rest as a validation set.

Method	SceneFlow EPE(px)	KITTI2015 (without finetuning) D1_all(%)
Switch training strategy Evaluation		
Relu(20 epochs)	0.9841	5.77
mish(20 epochs)	0.9379	5.67
mish(35 epochs)	0.8528	6.08
Relu(20 epochs)+ mish(15 epochs)	<b>0.7868</b>	<b>5.55</b>
Model setting Evaluation		
base	0.8578	6.18
MSNet	0.8387	5.81
MSMDNet	<b>0.7868</b>	<b>5.55</b>

Table 1: Ablation study results of our switch training strategy and model setting on SceneFlow test set and KITTI 2015 training set without finetuning.

## Implementation Details

we use pytorch to implement our network, and the whole network is trained in an end-to-end way with Adam ( $\beta_1 = 0.9, \beta_2 = 0.999$ ). Inspired by HSM-Net (Yang et al. 2019), we employ asymmetric chromatic augmentation and asymmetric occlusion for data augmentation. Switch training strategy is employed to train our model and it can be divided into three steps. First, we use Relu to train our network from scratch in SceneFlow dataset for 20 epochs. The initial learning rate is 0.001 and is down-scaled by 2 after epoch 12, 16, 18. Second, we use Mish to prolong the pre-training process in SceneFlow dataset for another 15 epochs. Third, we finetune our pre-trained model in KITTI 2015 and KITTI 2012 for another 400 epochs. The learning rate of this process begins at 0.001 and is decreased to 0.0001 after epoch 200. We only use the training images of KITTI 2012 for the fine-tuning process in KITTI 2012 while we merge the training images of both datasets for the fine-tuning process in KITTI 2015. The batch size is set to 4 for training on 2 NVIDIA V100 GPUs and the weight of six output is set as 0.5,0.5,0.5,0.7,1.0, and 1.3. The design principles of our switch training strategy will be discussed in the next section.

Method	2px(%)		3px(%)		4px(%)		5px(%)		runtime(s)
	Noc	All	Noc	All	Noc	All	Noc	All	
CSPN (Cheng, Wang, and Yang 2019)	1.79	2.27	1.19	1.53	0.93	1.19	0.77	0.98	1.0
AcfNet (Zhang et al. 2019b)	1.83	2.35	1.17	1.54	0.92	1.21	0.77	1.01	0.48
GANet-deep (Zhang et al. 2019a)	1.89	2.50	1.19	1.60	0.91	1.23	0.76	1.02	1.8
GwcNet (Guo et al. 2019)	2.16	2.71	1.32	1.70	0.99	1.27	0.80	1.03	<b>0.32</b>
SSPCVNet (Wu et al. 2019)	2.47	3.09	1.47	1.90	1.08	1.41	0.87	1.14	0.9
PSMNet (Chang and Chen 2018)	2.44	3.01	1.49	1.89	1.12	1.42	0.90	1.15	0.41
MSMD-Net	<b>1.69</b>	<b>2.18</b>	<b>1.04</b>	<b>1.37</b>	<b>0.78</b>	<b>1.01</b>	<b>0.63</b>	<b>0.81</b>	0.47

Table 2: Results on the KITTI 2012 benchmark.

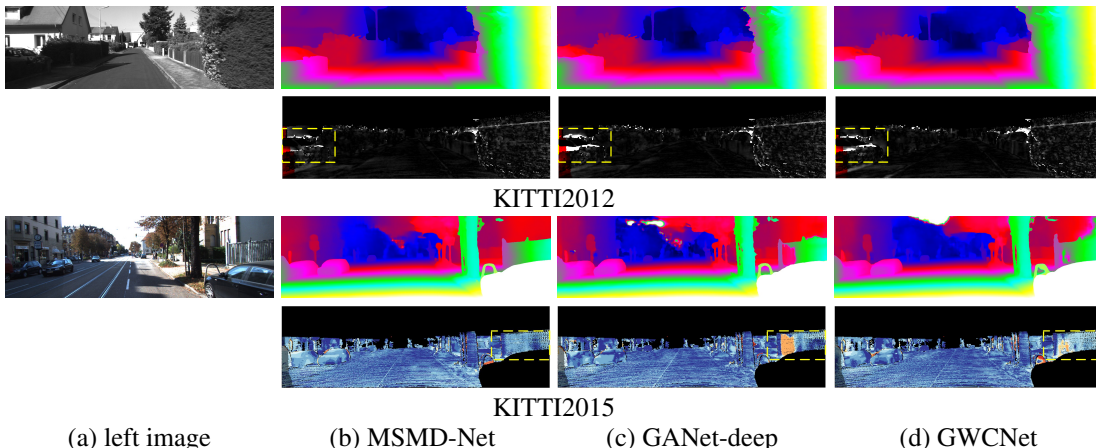


Figure 6: Visualization results on KITTI 2012 and KITTI 2015 testset. The left panel shows the left input image of stereo image pair, and for each example, the first row shows the predicted colored disparity map and the second row shows the error map.

### Switch Training Strategy

The activation function introduces non-linearity to the neural network and plays an integral role in the network performance. Relu (Hahnloser et al. 2000; Jarrett et al. 2009; Nair and Hinton 2010) and Swish (Ramachandran, Zoph, and Le 2017; Hayou, Doucet, and Rousseau 2018) are the two most widely used activation functions in the deep learning community. Recently, a new activation function, Mish (Misra 2019) is introduced and has shown its effectiveness in many challenging missions because of its properties of unbounded above, bounded below, smooth and non-monotonic (see supplementary material for the visualization comparison between Relu and Mish). As shown in Table 1 we also prove Mish is a better activation function in stereo matching compared with Relu by our experiment.

Prolonging the pre-training process in SceneFlow dataset is a general method to improve the performance for the final submission to the KITTI evaluation server. But such way seems useless when we employ Mish as activation function. We think some overfitting issues may arise because of the extension of the training process and the more effective optimization capacity of Mish compared with Relu. As shown in Table 1, This is also proved by a significant decline of EPE in SceneFlow dataset but poorer generalization ability on KITTI 2015 training set after the extension of the training process. Thankfully, the property of Mish makes it can directly replace activation functions like Relu without retraining a new model. So we propose a switch training strategy, which first uses Relu to get a pre-trained model in

SceneFlow dataset and then switch the activation function into Mish for the extension of the training process and use it to alleviate the issues discussed before. The effectiveness of our switch training strategy is proved by our experiment.

### Ablation Studies

In this section, we conduct ablation studies to evaluate the effectiveness of multiple scale cost volume and the refinement network with switch training strategy. Our base model is set as removing the cost volume integration module and the refinement network. MS-Net is added the cost volume integration module while MSMD-Net preserves our whole architecture. SceneFlow and KITTI 2015 (without pretraining from Scene Flow) datasets are used to evaluate our model. As shown in Table 1 and Table 4, the multiple scale cost volume and the refinement network significantly promoted the domain-across generalization and accuracy of disparity estimation.

We also conduct additional control experiments to analyze more specific model setting. In order to decrease training time, we only use KITTI 2015 dataset (without pretraining from Scene Flow) to do the control experiment. For the setting of multiple cost 3D aggregation, MS-Net is set as our control group. In the first model setting, we remove the blue lines in Figure 4, which means that we dont utilize the multi-scale cost volume. Such setting is equal to add one more stacked 3D hourglass network, so we call this new model base+. As shown in Table 4, the 3-pixel error rate improves 0.12% compared with MS-Net and is very similar

Method	All(%)			Noc(%)			Runtime(s)
	D1-bg	D1-fg	D1-all	D1-bg	D1-fg	D1-all	
CSPN (Cheng, Wang, and Yang 2019)	1.51	<b>2.88</b>	1.74	1.40	<b>2.67</b>	1.61	1.0
GANet-deep (Zhang et al. 2019a)	1.48	3.46	1.81	1.34	3.11	1.63	1.8
ACFNet (Zhang et al. 2019b)	1.51	3.80	1.89	1.36	3.49	1.72	0.48
CSN (Gu et al. 2020)	1.59	4.03	2.00	1.43	3.55	1.78	0.6
GWCNet (Guo et al. 2019)	1.74	3.93	2.11	1.61	3.49	1.92	0.32
SSPCVNet (Wu et al. 2019)	1.75	3.89	2.11	1.61	3.40	1.91	0.9
PSMNet (Chang and Chen 2018)	1.86	4.62	2.32	1.71	4.31	2.14	0.41
MSMDNet(only MS)	<b>1.41</b>	3.13	<b>1.69</b>	<b>1.29</b>	2.95	<b>1.57</b>	<b>0.32</b>

Table 3: Results on the KITTI 2015 benchmark.

Method	base	MS-Net	MSMD-Net
KITTI2015 Val Err (%)	2.08	1.94	<b>1.86</b>
Compare the setting of 3D aggregation			
Method	base+	MS-Net_small	MS-Net
KITTI2015 Val Err (%)	2.06	1.97	<b>1.94</b>
Compare of displacement setting			
Method	MSMD-Net_48	MSMD-Net_24	MSMD-Net_16
KITTI2015 Val Err (%)	1.97	<b>1.86</b>	1.90

Table 4: Additional model setting comparison on the KITTI 2015 dataset without pre-training

to our base model, which indicates the improvement of performance is not caused by the increase of training parameters and the importance of including multiple scale cost volumes. In the second model setting, we remove one stacked 3D hourglass network to maintain a close training parameter with GWCNet. This new model is denoted as MS-Net\_small. As shown in Table 4, the 3-pixel error rate improves 0.03% compared with MS-Net. Such result proves two stacked 3D hourglass network cant fully exploit the multiple scale information and it is necessary to add an additional cost volume integration module.

During the construction of warped correlation volume, the displacement is an essential hyper-parameter, which determines the disparity confidence range in the refinement network. So we also conduct a control experiment to compare the different settings of displacement. As shown in Table 4, 24 is the best setting and a larger setting will even give a negative influence to the network.

### Performance on KITTI Datasets

To further evaluate our model, we compare our proposed MSMD-Net with some existing state-of-the-art methods on KITTI 2012 and KITTI 2015 datasets.

For KITTI 2012, we submit the best trained MSMD-Net to the KITTI evaluation server. As shown in Table 2, our method reached a 1.37% overall three-pixel-error rate, which surpasses GWCNet (Guo et al. 2019) and SSPCVNet (Wu et al. 2019) by 0.33% and 0.53%, respectively. The closest method is ACFNet (Zhang et al. 2019b) while it cant get a comparable performance in KITTI 2015, which is 0.20% lower than ours.

For KITTI 2015, we find the refinement network cant give a significant improvement to the performance. In order to reduce the computation time, the best trained MS-Net is submitted to the KITTI evaluation server. As shown in Table 3, our method reached a 1.69% overall three-pixel-error rate which surpasses GWCNet and SSPCVNet by 0.42%. CSPN

(Cheng, Wang, and Yang 2019) is the best published method in KITTI 2015 and we can get a better result with 3 times faster speed. Figure 6 shows some result examples estimated by the proposed MSMD-Net, GWCNet, and GANet-deep (Zhang et al. 2019a) in KITTI 2012 and KITTI 2015 (more visualization examples can be seen in supplementary material). All results are downloaded from the KITTI evaluation server and our method shows significant improvement in ill-posed regions and fence region (see dash boxes in the picture).

### Cross-Domain Evaluation

In this section, we evaluate the cross-domain generalization of our model by training with synthetic data and testing on three real datasets. To make a fair comparison, all the methods are trained only on Scene Flow dataset (No additional synthetic dataset is used, i.e., Carla (Zhang et al. 2020)). As shown in Table 5, our method outperforms best prior works by a large margin on all three datasets with 3 times or even 5 times faster speed. Specifically, the error rate of KITTI 2012, KITTI 2015 and ETH3D is decreased 32.26%, 13.85% and 16.13%, respectively. Note that DSMNet (Zhang et al. 2020) is specially designed for cross-domain generalization but still cannot get a comparable result with our method, which shows that MSMD-Net can make a good balance between performance, speed and generalization.

Models	KITTI 2012(%)	KITTI 2015(%)	ETH3D(%)	time(s)
HD <sup>3</sup>	23.6	26.5	54.2	<b>0.14</b>
PSMNet	15.1	16.3	23.8	0.41
GWCNet	12.0	12.2	11.0	0.32
GANet	10.1	11.7	14.1	1.8
DSMNet	6.2	6.5	6.2	1.5
MSMDNet(only MS)	4.5	5.8	5.4	0.32
MSMDNet	<b>4.2</b>	<b>5.6</b>	<b>5.2</b>	0.47

Table 5: Generalization evaluation on KITTI 2012, KITTI2015 and ETH3D training images. Threshold error rates are used.

### Conclusion

In this paper, we have proposed MSMD-Net to construct multi-scale and multi-dimension cost volume. The 4D multi-scale combination volume is employed to better exploit multi-scale context information and the 3D warped correlation volume is used to generate a fine-grained disparity searching range for disparity refinement. We also introduce a switch training strategy to alleviate the overfitting issues during training. Experimental results show the superiority of

MSMD-Net across a diverse range of datasets. Specifically, MSMD-Net achieves state-of-the-art performance, strong domain-across generalization and efficient inference time at the same time. In the future, we plan to further extend our cost volume representation to other dense matching problems such as optical flow estimation and multi-view stereo.

## References

- Aleotti, F.; Tosi, F.; Zhang, L.; Poggi, M.; and Mattoccia, S. 2020. Reversing the cycle: self-supervised deep stereo through enhanced monocular distillation. *arXiv preprint arXiv:2008.07130*.
- Biswas, J.; and Veloso, M. 2011. Depth camera based localization and navigation for indoor mobile robots. In *RGB-D Workshop at RSS*, volume 2011, 21.
- Chang, J.-R.; and Chen, Y.-S. 2018. Pyramid stereo matching network. In *Proceedings of the IEEE Conference on Computer Vision and Pattern Recognition*, 5410–5418.
- Chen, C.; Seff, A.; Kornhauser, A.; and Xiao, J. 2015. Deep-driving: Learning affordance for direct perception in autonomous driving. In *Proceedings of the IEEE International Conference on Computer Vision*, 2722–2730.
- Cheng, S.; Xu, Z.; Zhu, S.; Li, Z.; Li, L. E.; Ramamoorthi, R.; and Su, H. 2019. Deep Stereo using Adaptive Thin Volume Representation with Uncertainty Awareness. *arXiv preprint arXiv:1911.12012*.
- Cheng, X.; Wang, P.; and Yang, R. 2019. Learning Depth with Convolutional Spatial Propagation Network. *IEEE transactions on pattern analysis and machine intelligence*.
- Duggal, S.; Wang, S.; Ma, W.-C.; Hu, R.; and Urtasun, R. 2019. DeepPruner: Learning Efficient Stereo Matching via Differentiable PatchMatch. In *Proceedings of the IEEE International Conference on Computer Vision*, 4384–4393.
- Geiger, A.; Lenz, P.; and Urtasun, R. 2012a. Are we ready for autonomous driving? the kitti vision benchmark suite. In *2012 IEEE Conference on Computer Vision and Pattern Recognition*, 3354–3361. IEEE.
- Geiger, A.; Lenz, P.; and Urtasun, R. 2012b. Are we ready for autonomous driving? the kitti vision benchmark suite. In *2012 IEEE Conference on Computer Vision and Pattern Recognition*, 3354–3361. IEEE.
- Gu, X.; Fan, Z.; Zhu, S.; Dai, Z.; Tan, F.; and Tan, P. 2020. Cascade cost volume for high-resolution multi-view stereo and stereo matching. In *Proceedings of the IEEE/CVF Conference on Computer Vision and Pattern Recognition*, 2495–2504.
- Guo, X.; Yang, K.; Yang, W.; Wang, X.; and Li, H. 2019. Group-wise correlation stereo network. In *Proceedings of the IEEE Conference on Computer Vision and Pattern Recognition*, 3273–3282.
- Hahnloser, R. H.; Sarpeshkar, R.; Mahowald, M. A.; Douglas, R. J.; and Seung, H. S. 2000. Digital selection and analogue amplification coexist in a cortex-inspired silicon circuit. *Nature* 405(6789): 947–951.
- Hayou, S.; Doucet, A.; and Rousseau, J. 2018. On the selection of initialization and activation function for deep neural networks. *arXiv preprint arXiv:1805.08266*.
- Jaderberg, M.; Simonyan, K.; Zisserman, A.; et al. 2015. Spatial transformer networks. In *Advances in neural information processing systems*, 2017–2025.
- Jarrett, K.; Kavukcuoglu, K.; Ranzato, M.; and LeCun, Y. 2009. What is the best multi-stage architecture for object recognition? In *2009 IEEE 12th international conference on computer vision*, 2146–2153. IEEE.
- Kendall, A.; Martirosyan, H.; Dasgupta, S.; Henry, P.; Kennedy, R.; Bachrach, A.; and Bry, A. 2017. End-to-end learning of geometry and context for deep stereo regression. In *Proceedings of the IEEE International Conference on Computer Vision*, 66–75.
- Liang, M.; Guo, X.; Li, H.; Wang, X.; and Song, Y. 2019a. Unsupervised Cross-Spectral Stereo Matching by Learning to Synthesize. In *Proceedings of the AAAI Conference on Artificial Intelligence*, volume 33, 8706–8713.
- Liang, Z.; Guo, Y.; Feng, Y.; Chen, W.; Qiao, L.; Zhou, L.; Zhang, J.; and Liu, H. 2019b. Stereo matching using multi-level cost volume and multi-scale feature constancy. *IEEE transactions on pattern analysis and machine intelligence*.
- Mayer, N.; Ilg, E.; Hausser, P.; Fischer, P.; Cremers, D.; Dosovitskiy, A.; and Brox, T. 2016. A large dataset to train convolutional networks for disparity, optical flow, and scene flow estimation. In *Proceedings of the IEEE Conference on Computer Vision and Pattern Recognition*, 4040–4048.
- Misra, D. 2019. Mish: A Self Regularized Non-Monotonic Neural Activation Function. *arXiv preprint arXiv:1908.08681*.
- Nair, V.; and Hinton, G. E. 2010. Rectified linear units improve restricted boltzmann machines. In *Proceedings of the 27th international conference on machine learning (ICML-10)*, 807–814.
- Pang, J.; Sun, W.; Ren, J. S.; Yang, C.; and Yan, Q. 2017. Cascade residual learning: A two-stage convolutional neural network for stereo matching. In *Proceedings of the IEEE International Conference on Computer Vision Workshops*, 887–895.
- Ramachandran, P.; Zoph, B.; and Le, Q. V. 2017. Searching for activation functions. *arXiv preprint arXiv:1710.05941*.
- Schops, T.; Schonberger, J. L.; Galliani, S.; Sattler, T.; Schindler, K.; Pollefeys, M.; and Geiger, A. 2017. A multi-view stereo benchmark with high-resolution images and multi-camera videos. In *Proceedings of the IEEE Conference on Computer Vision and Pattern Recognition*, 3260–3269.
- Sun, D.; Yang, X.; Liu, M.-Y.; and Kautz, J. 2018. Pwc-net: Cnns for optical flow using pyramid, warping, and cost volume. In *Proceedings of the IEEE Conference on Computer Vision and Pattern Recognition*, 8934–8943.
- Tonioni, A.; Tosi, F.; Poggi, M.; Mattoccia, S.; and Stefano, L. D. 2019. Real-time self-adaptive deep stereo. In *Pro-*

*ceedings of the IEEE Conference on Computer Vision and Pattern Recognition*, 195–204.

Wu, Z.; Wu, X.; Zhang, X.; Wang, S.; and Ju, L. 2019. Semantic Stereo Matching with Pyramid Cost Volumes. In *Proceedings of the IEEE International Conference on Computer Vision*, 7484–7493.

Yang, G.; Manela, J.; Happold, M.; and Ramanan, D. 2019. Hierarchical deep stereo matching on high-resolution images. In *Proceedings of the IEEE Conference on Computer Vision and Pattern Recognition*, 5515–5524.

Yang, J.; Mao, W.; Alvarez, J. M.; and Liu, M. 2020. Cost Volume Pyramid Based Depth Inference for Multi-View Stereo. In *Proceedings of the IEEE/CVF Conference on Computer Vision and Pattern Recognition*, 4877–4886.

Yu, F.; and Koltun, V. 2015. Multi-scale context aggregation by dilated convolutions. *arXiv preprint arXiv:1511.07122* .

Zhang, F.; Prisacariu, V.; Yang, R.; and Torr, P. H. 2019a. Ga-net: Guided aggregation net for end-to-end stereo matching. In *Proceedings of the IEEE Conference on Computer Vision and Pattern Recognition*, 185–194.

Zhang, F.; Qi, X.; Yang, R.; Prisacariu, V.; Wah, B.; and Torr, P. 2020. Domain-invariant Stereo Matching Networks. In *Europe Conference on Computer Vision (ECCV)*.

Zhang, Y.; Chen, Y.; Bai, X.; Zhou, J.; Yu, K.; Li, Z.; and Yang, K. 2019b. Adaptive Unimodal Cost Volume Filtering for Deep Stereo Matching. *arXiv preprint arXiv:1909.03751* .